

# Gamma-ray spectra resulting from the annihilation of positrons with selected core levels of Cu, Ag, and Au

S. Kim,<sup>1</sup> A. Eshed,<sup>1</sup> S. Goktepe,<sup>2</sup> P. A. Sterne,<sup>3</sup> A. R. Koymen,<sup>1</sup> W. C. Chen,<sup>1</sup> and A. H. Weiss<sup>1</sup>

<sup>1</sup>*Department of Physics, The University of Texas at Arlington, Arlington, Texas 76019, USA*

<sup>2</sup>*Motorola, 3501 Ed Bluestein Blvd., K10, Austin, Texas 78721, USA*

<sup>3</sup>*Lawrence Livermore National Laboratory, Livermore, California 94550, USA*

(Received 22 July 2005; published 26 January 2006)

The energy spectra of  $\gamma$  rays resulting from positron annihilation with selected core levels of Cu, Ag, and Au were obtained separately from the total annihilation spectra. The separation was accomplished by measuring the energy of  $\gamma$  rays detected in time coincidence with Auger electrons emitted consequent to the filling of holes resulting from the annihilation of core electrons. The results of these measurements are compared to the total annihilation spectra and with local-density approximation based theoretical calculations of the core contributions of the selected levels. Good agreement was found between calculated and measured values of the core momentum densities with no adjustable parameters outside of the overall normalization.

DOI: [10.1103/PhysRevB.73.014114](https://doi.org/10.1103/PhysRevB.73.014114)

PACS number(s): 61.72.-y, 71.60.+z, 78.70.Bj

## INTRODUCTION

Spectroscopies based upon the detection and analysis of the  $\gamma$  rays emitted when a positron becomes trapped and annihilates in a defect are among the most sensitive probes of open volume or charged defects in metals and semiconductors.<sup>1-3</sup> In addition, the tendency of positrons to become trapped at open volumes in polymers, at surfaces, at interfaces, and within nanoparticles has allowed positron-annihilation spectroscopy to be used as a highly selective probe of these systems.<sup>4-7</sup> The contributions to the Doppler-broadened annihilation spectra due to core electrons has become a subject of increased interest as the result of measurements demonstrating that it is possible to identify elements<sup>3,8</sup> from a chemically distinct spectral signature in the region of the  $\gamma$  spectra corresponding to core annihilation. In coincidence Doppler broadening (CDB) two Ge detectors are used to measure both the red and blue shifted annihilation  $\gamma$  rays in coincidence. The use of two detectors in coincidence has made it feasible to extract a statistically significant core annihilation contribution from the background resulting from the large valence contribution.<sup>9</sup> The CDB technique has been extensively applied in studies of vacancy-impurity complexes<sup>1-3</sup> and quantum dot nanoparticles and nanoprecipitates.<sup>5-7</sup>

In order to be confident in the elemental identification made using the coincidence-Doppler technique, it is important to understand the spectral contributions of the annihilation with core electrons in detail. However the core contributions constitute only a small fraction of the total spectrum due to the fact that, typically, more than 90% of the annihilation events occur with the valence electrons due to the repulsion of positron from the positive core. This makes it impossible, using only  $\gamma$  detection, to uniquely identify the core contributions to the spectra. Recently, Eshed *et al.*<sup>10</sup> reported measurements of the Doppler-broadened  $\gamma$ -ray energy spectra associated with the annihilation of a positron with selected core levels of Cu and Ag using a technique in which  $\gamma$  rays are detected in coincidence with Auger elec-

trons. In this paper we report research expanding on this previous work and report data on the Doppler-broadened  $\gamma$ -ray energy spectra associated with the annihilation of a positron with the core levels of Au. The core annihilation spectra for Au is compared to data obtained for Cu and Ag. An analysis applied to all three sets of data yielded improved agreement with local-density approximation (LDA) calculations of the core momentum densities by taking into account the contributions from deeper cores due to the Auger cascade process. We also present a detailed discussion of the experimental system used in the  $\gamma$ -Auger coincidence measurements and the methods used in extracting the pair momentum densities from the Doppler broadened  $\gamma$  spectra. The Auger-coincidence methods, described in this paper, can be applied in other types of momentum measurements including angular correlation of annihilation radiation (ACAR) and to study the effects of adsorbates and reduced coordination on the core level momentum densities of atoms at the surface.

The experimental measurements of the annihilation  $\gamma$  spectra for core levels reported in this paper provide a stringent test of theoretical calculations of core annihilation momentum distributions, and a guide to the construction of improved descriptions of the electron-positron correlation effects as they pertain to annihilation with core electrons. The addition of the Au data to that obtained for Cu and Ag has allowed us to test if LDA-based theory adequately accounts for the ratio of high momentum to low momentum spectral weight in the extracted momentum densities for cores with increasing principal quantum number. It was found that excellent agreement could be obtained between theory and experiment for Au and Cu when the contributions of all core annihilations events that lead to Auger electron emission in the appropriate energy range are included. The agreement between the data, which were obtained from the annihilation of surface state positrons, and the theory, which was calculated for annihilation of a positron in a spherical state around the atom, indicate that positron wave function effects do not cause serious problems in calculating momentum densities for core electrons.

## BACKGROUND

Positrons in solids annihilate predominantly into two  $\gamma$  rays. In the center of mass frame these  $\gamma$  rays are emitted equal in energy and opposite in propagation direction. In the laboratory frame, the center of mass motion of the positron-electron pair results in a Doppler shift of magnitude,  $(P_L c)/2$ , yielding energies,  $E_{\gamma 1}$  and  $E_{\gamma 2}$  for the two annihilation  $\gamma$  rays:

$$\begin{aligned} E_{\gamma 1} &= m_0 c^2 - E_B/2 + (P_L c)/2, \\ E_{\gamma 2} &= m_0 c^2 - E_B/2 - (P_L c)/2. \end{aligned} \quad (1)$$

Where  $m_0$  is the rest mass of the electron (positron),  $c$  is the speed of light,  $E_B$  is the binding energy of the electron, and  $P_L$  is the component of the center of mass momentum of the electron-positron pair along the direction of the  $\gamma$ -ray emission. Equation (1) can be inverted to obtain the momentum of the electron-positron pair at the time of annihilation in the direction of the HPGe  $\gamma$  detector<sup>15-17</sup>

$$P_L = \frac{2E_{\gamma 1} - 2m_0 c^2 + E_B}{c}. \quad (2)$$

As a consequence, a histogram of the energy of detected annihilation  $\gamma$ 's can be used to obtain a one-dimensional projection of the momentum distribution of annihilating electron-positron pairs. This distribution can be modeled by appropriate two-dimensional integration of a calculated momentum distribution given by

$$\rho(\mathbf{p}) = \pi r_0^2 c \sum_i \left| \int d\mathbf{r} e^{i\mathbf{p}\cdot\mathbf{r}} \Psi^+(\mathbf{r}) \Psi_i^-(\mathbf{r}) [\Gamma_i(\mathbf{p}, \mathbf{r})]^{1/2} \right|^2, \quad (3)$$

where  $\mathbf{r}_0$  is the classical electron radius,  $\mathbf{p}$  is the total momentum of the annihilation pair, and  $\Psi^+(\mathbf{r})$  is the positron wave function  $\Psi_i^-(\mathbf{r})$  is the wave function for the  $i$ th electron and  $\Gamma_i(\mathbf{p}, \mathbf{r})$  is a weighting function that models "enhancement" i.e., electron-positron correlation affects which lead to an annihilation rate higher than that predicted in the independent particle approximation.<sup>11</sup>

Calculations of the annihilation  $\gamma$  spectra with sufficient accuracy to extract chemical information in positron defect studies require a detailed understanding of the enhancement factor,  $\Gamma_i(\mathbf{p}, \mathbf{r})$ , for core levels. Conventional measurements (including those using  $\gamma$ - $\gamma$  coincidence techniques<sup>3,8,9</sup>) probe the total momentum density of the system including both core and valence electrons. In modeling this data, Eq. (3) must be summed over all occupied electron states. Thus conventional spectra must be compared with calculations of sums of individual level momentum densities weighted by momentum dependent enhancement factors that introduce uncertainties that seriously limit the reliability of the comparison.

The  $\gamma$  spectra obtained using the  $\gamma$ -Auger coincidence technique make it possible to compare the measured and model momentum distributions of selected core levels and provide a unique means to test theoretical efforts to go beyond the local density approximation (LDA), (which can be expected to break down for the core levels because of their

wide range of momenta and large electron density gradients<sup>12</sup>), such as the generalized gradient approximation (GGA) (Ref. 13) and explicitly non-local treatments<sup>12</sup> such as the weighted density approximation (WDA). In addition, the  $\gamma$ -Auger coincidence measurements provide the only means available, to date, of measuring the low momentum part of the annihilation spectra for cores (the low momentum contribution of the cores is swamped by valence band annihilation using  $\gamma$  spectroscopy alone). The measurement of the low momentum part of the spectra of the cores makes it possible to determine the ratio of the high momentum to low momentum contributions providing a test of attempts to model the momentum dependence of  $\Gamma$ .<sup>14</sup>

## EXPERIMENT

The method of selecting  $\gamma$  rays associated with the annihilation of core electrons relies on the fact that an energetic core hole left by the annihilation event can decay via the almost simultaneous emission of one or more Auger electron(s) with energies characteristic of the core level(s).<sup>15,16</sup> For the outer core levels (the levels of most relevance to Doppler broadening measurements) almost all the core hole excitations decay via Auger processes.<sup>17,18</sup> For example, in a core-valence-valence Auger process, a valence electron carries off the energy made available when another valence electron fills the core hole left by annihilation. Previous measurements have demonstrated that it is possible to detect annihilation-induced Auger electrons with high efficiency and with an energy resolution sufficient to infer the energy levels of the initial core holes.<sup>15,16</sup> As a result,  $\gamma$  spectra associated with positron annihilation with electrons in selected core levels can be obtained by measuring the energies of  $\gamma$ 's detected in coincidence with annihilation-induced Auger electrons of the appropriate energy.

The  $\gamma$ -Auger coincidence data were collected using a magnetically guided positron beam system described previously.<sup>19</sup> The measurements were performed using a positron beam energy of 12 eV and a flux of  $\sim 2 \times 10^4$  positrons/second. The beam system is equipped with a trochoidal energy analyzer which is used for Positron annihilation-induced Auger spectroscopy, an ion-sputter gun and a conventional electron stimulated Auger system (PHI-1100) (the later two systems are operated with the magnetic field of the positron beam turned off). The previous configuration of the beam system was augmented with the addition of a HPGe detector (ORTEC-GEM-30185P, 58.6 mm diam.  $\times$  54.8 mm, relative efficiency 32% at 1.33 MeV), which was mounted perpendicular to the positron beam, 0.058 m from the sample, and behind a 0.0016 m stainless steel vacuum window. The full width at half maximum (FWHM) of the detector resolution was measured to be 1.23 keV at 514 keV using a <sup>85</sup>Sr calibration source.

The samples were cut to a size of 20 mm  $\times$  20 mm from pure Ag, Cu, and Au foils, etched in a 48% solution of hydrofluoric acid and rinsed in acetone and ethyl alcohol before loading into the vacuum chamber which was evacuated and

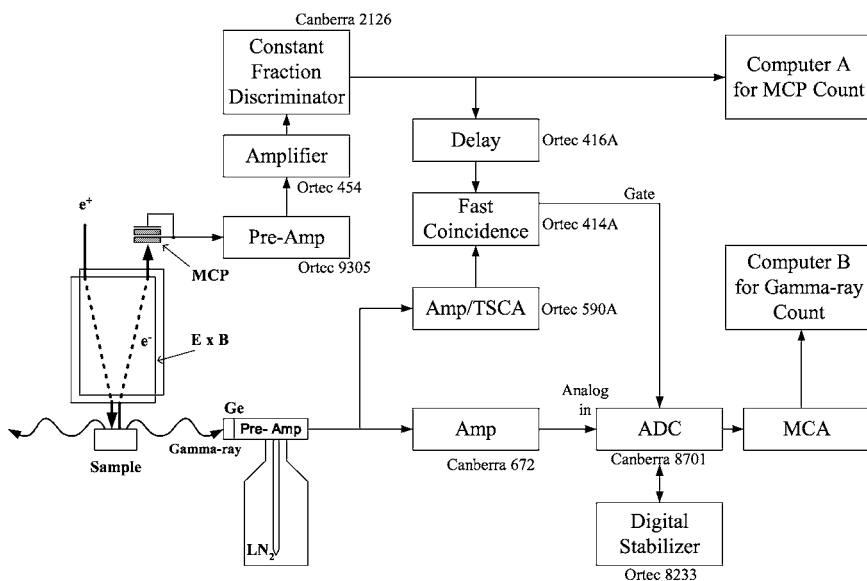


FIG. 1. Details of the experimental setup. A low energy positron beam is used to place positrons at the sample surface. The signal from the preamp of the HPGe  $\gamma$  detector is amplified and connected to the ADC of a multichannel analyzer (MCA). The Auger electrons were energy selected using an  $E \times B$  filter and detected using a microchannel plate (MCP). The Doppler-broadened  $\gamma$  spectrum for a selected core level was acquired by using a fast coincidence circuit to open the gate to the MCA only after the simultaneous detection of a  $\gamma$  ray and an electron from the selected Auger transition. Conventional Doppler-broadened spectra were acquired by holding the MCA gate open.

baked to obtain UHV conditions. The samples were initially cleaned by repeated sputter-anneal cycles (30 min sputtering by neon (Ag) or argon (Cu, Ag, Au) ions followed by annealing at  $\sim 150^\circ\text{C}$ . The sample was maintained under UHV conditions and sputtered for 3 h two times a week during the period of data acquisition ( $\sim 20$  days per sample). Surface cleanliness was monitored throughout the  $\sim 20$  day period required for data accumulation by conventional electron stimulated Auger spectroscopy (EAES) and contamination levels were observed to be below 1% except for C and O for which the surface concentration stayed below 10% during the data collection period. We note that the spectral weight in the energy range of interest from the low energy tails of the annihilation-induced C (O) Auger lines for 100% C (50% O) surfaces are only a few percent of the positron annihilation induced Auger intensities of Cu, Ag, and Au.<sup>20</sup> Consequently, we estimate that less than 0.2% of the  $\gamma$ -Auger coincidence signal is from the C and O cores.

The  $\gamma$ -Auger coincidence spectra (containing contributions only from core annihilation) were obtained by gating the input from the HPGe detector into the multichannel analyzer (MCA) with a pulse resulting from the detection of electron in the selected energy range within 600 ns of the detection of the  $\gamma$ -ray (see Fig. 1). Conventional “non-coincidence”  $\gamma$ -spectra (containing contributions from both core and valence annihilation) were obtained by setting the gate input high allowing all of the HPGe pulses into the MCA.

The annihilation  $\gamma$  spectra of the core levels (levels with binding energies greater than or equal to that of the  $3p$  level) of Cu were obtained by requiring coincidence with electrons in the energy range 57–59 eV. This range spans the peak of the energy distribution of the  $M_{23}VV$  Auger transition. Similarly the annihilation  $\gamma$  spectra of the core levels (levels with binding energies greater than or equal to that of the  $4p$  level) of Ag were obtained by requiring coincidence with electrons in the energy range 35–38 eV (corresponding to the Ag  $N_{23}VV$  Auger transition) and the annihilation  $\gamma$  spectra of the core levels (levels with binding energies greater than or equal to that of the  $5p$  level) for Au were obtained by requir-

ing coincidence with electrons in the range 38–40 eV for Au (corresponding to the Au  $O_{23}VV$  Auger transition).

A small background (accounting for 5.4% of the total intensity for Cu, 11.6% for Ag, and 5.5% for Au) due to accidental coincidences between the  $\gamma$  signal and uncorrelated pulses from the microchannel plate (MCP) was determined directly from a measurement of the integrated intensity of the  $\gamma$  signal taken in coincidence with electrons detected in an energy range where no true coincidences are present (20 eV above the annihilation-induced Auger peak). The accidental contribution was then removed by subtracting a high statistics, noncoincidence  $\gamma$  spectra scaled to match the measured intensity of the accidental contribution to the spectra. Figure 2 shows a comparison of the  $\gamma$ -Auger coincidence data associated with the annihilation of positrons with Cu  $3p$  electrons before and after subtraction of the accidental background.

We note that the kinetic energy of the positrons hitting the surface at 12 eV, was below the impact-ionization threshold for all of the core levels studied. This was important to en-

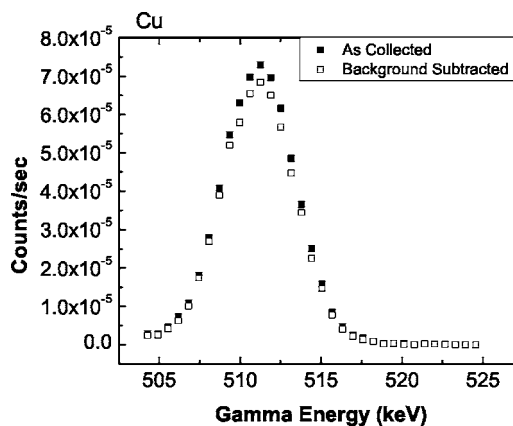


FIG. 2. Comparison of  $\gamma$ -ray -Auger electron coincidence data from a Cu surface as collected and the same data with the accidental background subtracted. The  $\gamma$  spectra were obtained by impinging 12 eV positrons on a Cu surface and taken in coincidence with the detection of electrons in the Cu  $M_{23}VV$  Auger peak.

sure that the Auger electrons detected resulted from annihilation with core electron and not from Auger electrons resulting from impact ionization. If a positron beam-energy higher than the core ionization energy was to be used, it would excite Auger electrons both by positron annihilation with core electrons and by impact ionization. The use of too high a positron-beam energy would also result in positron-induced secondary electrons with energies in the range of the Auger electrons.<sup>21</sup> Since the positrons that cause impact ionization or impact-induced secondaries are free to annihilate with valence electrons after the impact, the presence of Auger electrons (or secondary electrons) in the Auger energy range from impact excitation would result in an undesirable valence background in the coincidence measurements. Note also that a large fraction of the positrons injected into the samples at 12 eV diffuse back to the surface and become trapped in an image correlation well before they annihilate. This greatly increases the escape probability of the Auger electrons and implies that the  $\gamma$ -Auger coincidence technique predominantly samples atoms in the topmost atomic layer.

### THEORETICAL CALCULATIONS

The calculations were based on an atomic code using a local-density form for the electron-positron correlation function.<sup>22</sup> The calculations include appropriate integration of the three-dimensional (3D) radial momentum distribution to correspond to the 1D Doppler measurements. We use an approach in which the momentum integration is performed analytically using a  $\delta$ -function identity, thereby reducing the expression for the 1D momentum density to real-space integrals over well-behaved radial functions. As a result of the integration, nodes in the radial momentum distributions result in breaks in momentum that appear as shoulders in the 1D momentum distribution.

The calculations use a generalized-gradient approximation (GGA) for the electron-positron enhancement.<sup>23</sup> Separate calculations were performed using state-dependent and  $r$ -dependent enhancement. State-dependent enhancement uses a constant, momentum-independent enhancement factor equal to the average enhancement of the individual atomic state, corresponding to  $\Gamma_i(\mathbf{p}, \mathbf{r}) = \gamma_i$  in Eq. (3). In  $r$ -dependent enhancement, the enhancement factor in  $\Gamma_i(\mathbf{p}, \mathbf{r})$  Eq. (3) is replaced by a density-dependent enhancement factor,  $\gamma[n(r)]$  prior to performing the radial integrations to produce the 1D momentum density, resulting in a momentum-dependent enhancement function.

The electron-positron enhancement function  $\gamma[n(r)]$  becomes very large when the density becomes small. In our atomic calculation, the electron charge density drops off rapidly at large radii, while in a real solid the charge density from the neighboring atoms would maintain a much larger charge density. For this reason, we limit the enhancement to a value determined by the interstitial charge density in each of the elements we consider here, with  $r_s$  values of 2.67, 3.02, and 3.0, respectively, for Cu, Ag, and Au.

### RESULTS AND DISCUSSION

Figure 3(a) shows a comparison of the energy distribution of annihilation  $\gamma$  rays from positrons incident on Cu mea-

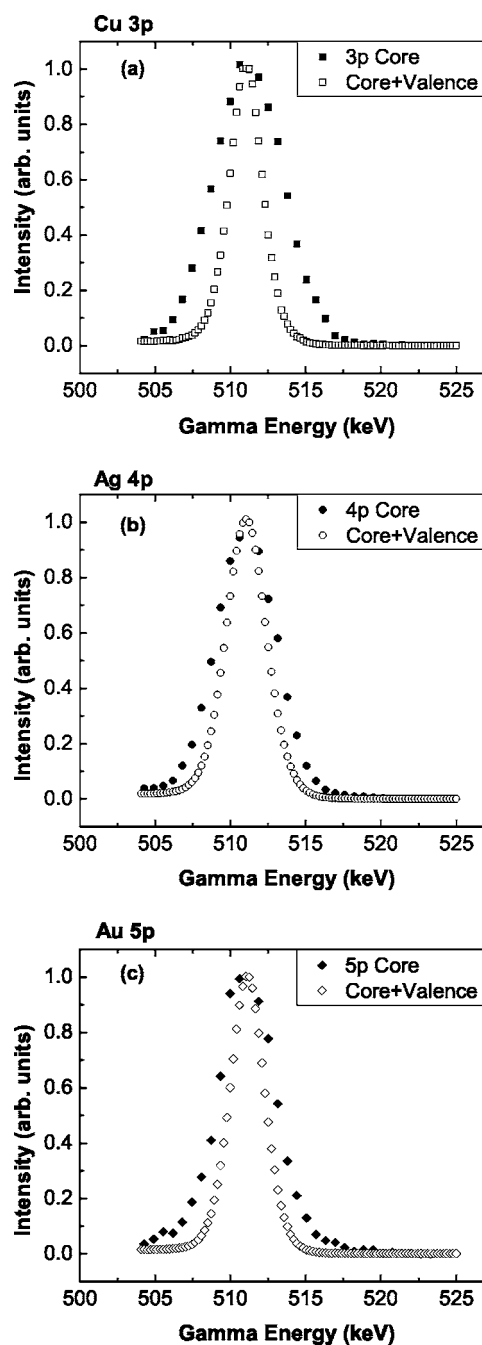


FIG. 3. Comparison of the core + valence and core annihilation  $\gamma$ -ray energy spectra resulting from the bombardment of polycrystalline Cu (a), Ag (b), and Au (c) foils with a 12 eV positron beam. The core + valence spectra (open symbols) were acquired without a coincidence requirement. The core spectra (solid symbols) were acquired in time coincidence with the detection of an electron in the range of the peaks of the energy distribution of Auger electrons emitted as a result of transitions involving an initial hole in the Cu 3p ( $M_{23}$ ), Ag 4p ( $N_{23}$ ), and Au 5p ( $O_{23}$ ) levels for panels (a), (b), and (c), respectively.

sured in coincidence with an Auger electron emitted as a result of filling the 3p core hole in Cu with a spectra obtained without the requirement of coincidence. Similarly, panels 3(b) and 3(c) show comparisons of the energy spectra



of annihilation  $\gamma$  rays obtained with and without the requirement for coincidence with Auger electrons emitted as a result of filling the  $4p$  level in Ag and the  $5p$  level in Au, respectively. All the data sets shown in Fig. 3 were scaled such that they coincide at the peak.

In all three cases the widths of the coincidence spectra are significantly larger than those of the non-coincidence spectra. The full width at half maximum (FWHM) of the noncoincidence spectra are 2.24, 2.73, and 2.38 keV from Cu, Ag, and Au, respectively, while the corresponding FWHM of the coincidence spectra are 5.5, 4.6, and 4.4 keV, respectively. This is consistent with the fact that the noncoincidence data are dominated by  $\gamma$ 's resulting from annihilation with the relatively low momentum valence electrons and the coincidence data characterizes the energy spectra of  $\gamma$  rays emitted as a result of annihilation with relatively high momentum core electrons.

A qualitative understanding of the spectral widths of the noncoincidence spectra can be obtained by estimating the width of the momentum distribution of the valence electrons alone. To the lowest approximation this contribution can be modeled by a parabola representing annihilation with free conduction electrons. The parabola cuts off at an energy  $\Delta E_{\max}$

$$\Delta E_{\max} = m_0 c^2 \frac{V_F}{2c} \approx 1 \text{ KeV} \quad (4)$$

where  $V_F$  is the Fermi velocity of an electron ( $\sim 10^6 \text{ ms}^{-1}$ ).<sup>15-17</sup>

The larger width of the coincidence spectra is due to the relatively large Doppler shift associated with the core electrons which are the sole contributors to the coincidence spectra. As noted above, the FWHM of the coincidence spectra are 5.5, 4.6, and 4.4 keV from the Cu  $3p$ , Ag  $4p$ , and Au  $5p$  levels, respectively. The ratios of these widths, 1.25:1.05:1, correspond approximately to the ratios of the square root of the binding energies of the  $p^{3/2}$  levels (a rough estimate of the ratios of the magnitudes of momentum of these levels) 1.15:1.01:1. The fact that the Au  $5p$  is less tightly bound than the Ag  $4p$  which in turn is less tightly bound than the Cu  $3p$  implies that the Au  $5p$  is wider in real space than the Ag  $4p$  which is again wider than the Cu  $3p$  and hence their widths in momentum space are reversed.

We note that the use of  $\gamma$ -Auger coincidence, like the use of  $\gamma$ - $\gamma$  coincidence eliminates background due to Ps, nuclear decay and cosmic ray  $\gamma$ 's, etc. However, only  $\gamma$ -Auger coincidence is capable of separating the core part of the annihilation spectra from the much larger (20 times at the peak) valence contribution.

Figure 4 shows a comparison between measurements made using the Auger- $\gamma$  coincidence technique and first principles calculations of the one-dimensional projection of the momentum distribution of annihilating electron-positron pairs of core electrons determined using the methods described above with state-dependent enhancement. The momentum is expressed in dimensionless atomic units, where  $q$  is the wave vector and  $a_0$  is the Bohr radius. The calculated values are the result of summing the intensities of the mo-

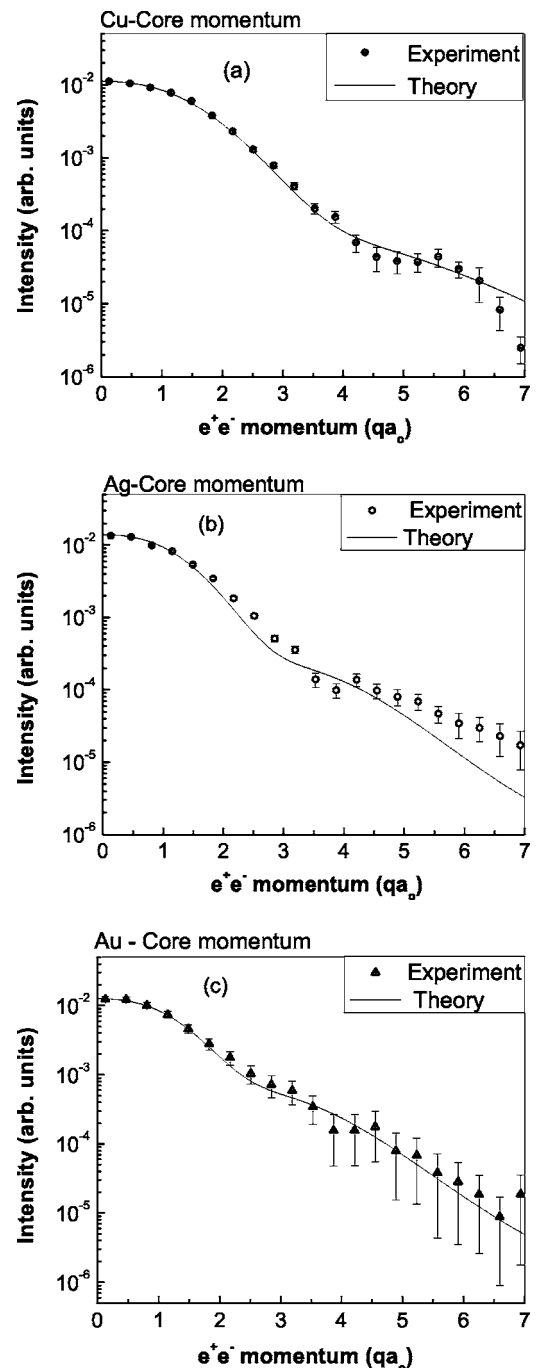


FIG. 4. Momentum distributions of the positron-electron pairs involved in the annihilation of positrons with the core levels of Cu (a), Ag (b), and Au (c). The experimental distributions (solid squares) were extracted from the Doppler-broadened spectra by using Eq. (2). The measured distributions are compared to LDA-based calculations normalized to have the same value at the peaks.

mentum distribution for all core levels with binding energies greater than or equal to those of the  $3p$  in Cu, the  $4p$  in Ag, and the  $5p$  in Au. We note that we have modified the analysis used previously in Ref. 10, in which only the contribution from the outer core was included, by including the contribution from the deeper core levels. The previous analysis assumed that all the (MVV) Auger transitions in Cu and

(NVV) Auger transitions in Ag were preceded by annihilation with M shell electrons in Cu and N shell electrons in Ag, respectively. This assumption neglects the contribution to annihilation spectra from events in which  $\gamma$  rays emitted from deeper core levels are detected in coincidence with Auger electrons emitted in a cascade process.<sup>24</sup> For example, the annihilation of an electron in the L shell of Cu can result in a MVV Auger transition via the cascade process in which a LMV or LMM transition is followed by a MVV Auger transition. Although such processes account for only a small fraction of the electrons emitted in the energy range of the Cu MVV peak (which are overwhelmingly electrons emitted in a direct Auger transitions in which the positron annihilates with electrons in the M shell), the contribution of coincidence events involving cascade processes is significant in the high momentum region of the  $\gamma$  spectra. This follows from the fact that the high momentum region of the total annihilation spectra is dominated by contributions from annihilation with the deeper cores due to the high momentum of the core electrons even though the probability for such annihilation events is low due to core repulsion together with the fact that holes in the deep core level are converted into holes in the outer cores with high efficiency.<sup>24</sup> Consequently the spectral contribution of annihilation events involving the deeper holes needs to be included in order to accurately model the coincidence data in the high momentum region. We note that contributions from individual core levels could be obtained by comparing a sequence of  $\gamma$  spectra taken in coincidence with higher and higher energy Auger peaks.

The agreement between theory and experiment is remarkable given the complexities of both the experiment and theory and the fact that the calculations were done independently with no adjustable parameters aside from the overall normalization. Referring to Fig. 4 panels 4(a) and 4(c), it may be seen that the agreement between theory and experiment is within the limits of statistical uncertainty for Cu and Au. However, referring to panel 4(b) it may be seen that there are differences between theory and experiment for Ag that are outside of the statistical uncertainties of the experiment. Specifically, when both theory and experiment are set to be equal at the peak, the calculation for Ag lies consistently below the experimental values for  $qa_0 > 3$ . Because the normalization procedure made the measured and theoretical values coincide in the low momentum part of the spectra, some care should be taken in assuming the comparison indicates that the discrepancy between theory and experiment is only at high momentum.

There are a number of possible explanations for the discrepancies between theory and experiment in Ag: (1). Auger cascade processes lead to a larger relative contribution of annihilation events with deeper cores in Ag than in the case of Cu and Au. We note however that modeling of the data indicates that in order to get better agreement, the contributions from coincidence events involving annihilation with deeper cores would need to be much larger for Ag than for Cu or Au, while the Auger cascade processes should have similar efficiencies for all three metals. (2). The LDA-based calculation of the core electron momentum distribution may underestimate the high momentum tails. However, while the LDA is known to give the wrong core level binding energies,

the charge densities from which the momentum distributions are calculated are believed to be accurate. (3). The discrepancies may be due to the level of approximation used in modeling the positron wave function in which only a  $s$ -like state was included. While  $s$  states have appeared to be adequate for approximating the positron state in bulk calculations, it is likely that a mixed  $s$ - $p$  state may be more appropriate for the overlap of a positron in a surface state with a surface atom. We note however, that the observed discrepancies appear to be in the high momentum region in which the positron's contribution to the total pair momentum could be expected to be small due to the fact that, on the average, the positrons are at thermal energies at the time of annihilation. (4). The discrepancy may reflect inadequacies in the treatment of electron-positron correlation effects and the need for an enhancement term with an explicit momentum dependence that increases at higher momentum. We note, however, that current treatments of the momentum dependence of the LDA based theories predict the opposite momentum dependence, and our  $r$ -dependent enhancement factor calculations, which introduce a momentum-dependent enhancement factor, in fact showed a preferential enhancement of the low-momentum electrons, further worsening the agreement with experiment for Ag.

## CONCLUSIONS

The data presented in this paper represents the results of the first measurements of the Doppler-broadened  $\gamma$ -ray spectra resulting from the annihilation of positrons with individual core levels. Annihilation  $\gamma$  spectra from selected core levels in Cu, Ag, and Au were obtained by measuring the energies of  $\gamma$ -rays time coincident with Auger electrons emitted as a result of positrons annihilating with a core level. A comparison with calculations of the annihilation spectra for the core levels shows excellent qualitative agreement with no adjustable parameters aside from the overall normalization. However, differences with theory are well outside of the statistical uncertainties for Ag.

We note that our measurements directly separate the low momentum contributions of the core from the much larger signal from annihilation with valence electrons. The method of using coincidence with the detection of Auger electrons to select core annihilation events, while used in this study to measure the Doppler broadened  $\gamma$  spectra, is of general applicability in studies of core annihilation. Future  $\gamma$ -Auger coincidence measurements could be used to measure the core spectra of impurity atoms at the surface. The core signatures of impurities thus obtained could then be used to provide confirmation of the signatures of vacancy-impurity complexes in the bulk as seen in Doppler spectra obtained using  $\gamma$ - $\gamma$  coincidence. The Auger coincidence technique can also be used in conjunction with the measurement of the angular correlation of annihilation radiation, (ACAR), in high-resolution fundamental studies of core electron momentum distributions.

## ACKNOWLEDGMENTS

This work was supported in part by the NSF DMR-9812628 and The Welch Foundation Grant Nos. Y-1100 and

Y-1215. Part of this work was performed under the auspices of the U.S. Department of Energy by the University of California, Lawrence Livermore National Laboratory under Contract No. W-7405-Eng-48.

- 
- <sup>1</sup>M. Rummukainen, I. Makkonen, V. Ranki, M. J. Puska, K. Saarinen, and H. -J. L. Gossmann, *Phys. Rev. Lett.* **94**, 165501 (2005).
- <sup>2</sup>M. P. Petkov, M. H. Weber, K. G. Lynn, R. S. Crandall, and V. J. Ghosh, *Phys. Rev. Lett.* **82**, 3819 (1999).
- <sup>3</sup>M. Alatalo, H. Kauppinen, K. Saarinen, M. J. Puska, J. Mäkinen, P. Hautojärvi, and R. M. Nieminen, *Phys. Rev. B* **51**, 4176 (1995).
- <sup>4</sup>D. W. Gidley, W. E. Frieze, T. L. Dull, J. Sun, A. F. Yee, C. V. Nguyen, and D. Y. Yoon, *Appl. Phys. Lett.* **76**, 1282 (2000).
- <sup>5</sup>Jun Xu, A. P. Mills, Jr., A. Ueda, D. O. Henderson, R. Suzuki, and S. Ishibashi, *Phys. Rev. Lett.* **83**, 4586 (1999).
- <sup>6</sup>X. Y. Zhang, Y. Guan, and J. W. Zhang, *Appl. Phys. Lett.* **80**, 1966 (2002).
- <sup>7</sup>Y. Nagai, M. Hasegawa, Z. Tang, A. Hempel, K. Yubuta, T. Shimamura, Y. Kawazoe, A. Kawai, and F. Kano, *Phys. Rev. B* **61**, 6574 (2000).
- <sup>8</sup>P. Asoka-Kumar, M. Alatalo, V. J. Ghosh, A. C. Kruseman, B. Nielsen, and K. G. Lynn, *Phys. Rev. Lett.* **77**, 2097 (1996).
- <sup>9</sup>K. G. Lynn, J. E. Dickman, W. L. Brown, M. F. Robbins, and E. Bonderup, *Phys. Rev. B* **20**, 3566 (1979).
- <sup>10</sup>A. Eshed, S. Goktepe, A. R. Koymen, S. Kim, W. C. Chen, D. J. O'Kelly, P. A. Sterne, and A. H. Weiss, *Phys. Rev. Lett.* **89**, 075503 (2002).
- <sup>11</sup>M. Alatalo, B. Barbiellini, M. Hakala, H. Kauppinen, T. Korhonen, M. J. Puska, K. Saarinen, P. Hautojärvi, and R. M. Nieminen, *Phys. Rev. B* **54**, 2397 (1996).
- <sup>12</sup>A. Rubaszek, Z. Szotek, and W. M. Temmerman, *Phys. Rev. B* **58**, 11285 (1998).
- <sup>13</sup>B. Barbiellini, M. Hakala, M. J. Puska, R. M. Nieminen, and A. A. Manuel, *Phys. Rev. B* **56**, 7136 (1997).
- <sup>14</sup>B. B. J. Hede and J. P. Carbotte, *J. Phys. Chem. Solids* **33**, 727 (1972).
- <sup>15</sup>A. Weiss, R. Mayer, M. Jibaly, C. Lei, D. Mehl, and K. G. Lynn, *Phys. Rev. Lett.* **61**, 2245 (1988).
- <sup>16</sup>A. H. Weiss and P. G. Coleman, in *Positron Beams and Their Applications*, edited by Paul Coleman (World Scientific, Singapore, 2000), pp. 152–165.
- <sup>17</sup>E. J. McGuire, *Phys. Rev. A* **5**, 1052 (1972).
- <sup>18</sup>D. Briggs and M. P. Seah, *Practical Surface Analysis* (Wiley, New York, 1994), p. 92.
- <sup>19</sup>C. Lei, D. Mehl, A. R. Koymen, F. Gotwald, M. Jibaly, and A. H. Weiss, *Rev. Sci. Instrum.* **60**, 3656 (1989).
- <sup>20</sup>J. G. Zhu, M. P. Nadesalingam, A. H. Weiss, and M. Tao, *J. Appl. Phys.* **97**, 103510 (2005); Shuping Xie, Ph.D. dissertation, University of Texas at Arlington, (2002).
- <sup>21</sup>A. Weiss, D. Mehl, A. R. Koymen, K. H. Lee, and Chun Lei, *J. Vac. Sci. Technol. A* **8**, 2517 (1990).
- <sup>22</sup>P. A. Sterne, P. Asoka-Kumar, and R. H. Howell, *Appl. Surf. Sci.* **194**, 71 (2002).
- <sup>23</sup>B. Barbiellini, M. J. Puska, T. Torsti, and R. M. Nieminen, *Phys. Rev. B* **51**, 7341 (1995); B. Barbiellini, M. J. Puska, T. Korhonen, A. Harju, T. Torsti, and R. M. Nieminen, *ibid.* **53**, 16201 (1996).
- <sup>24</sup>Max Wolfsberg and Morris L. Perlman, *Phys. Rev.* **6**, 1833 (1955).